A strategy for the eigenvector perturbations of the Reynolds stress tensor in the context of uncertainty quantification

By R. L. Thompson†, L. E. B. Sampaio, W. Edeling, A. A. Mishra AND G. Iaccarino

In spite of increasing progress in high fidelity turbulent simulation avenues like Direct Numerical Simulation (DNS) and Large Eddy Simulation (LES), Reynolds-Averaged Navier-Stokes (RANS) models remain the predominant numerical recourse to study complex engineering turbulent flows. In this scenario, it is imperative to provide reliable estimates for the uncertainty in RANS predictions. In the recent past, an uncertainty estimation framework relying on perturbations to the modeled Reynolds stress tensor has been widely applied with satisfactory results. Many of these investigations focus on perturbing only the Reynolds stress eigenvalues in the Barycentric map, thus ensuring realizability. However, these restrictions apply to the eigenvalues of that tensor only, leaving the eigenvectors free of any limiting condition. In the present work, we propose the use of the Reynolds stress transport equation as a constraint for the eigenvector perturbations of the Reynolds stress anisotropy tensor once the eigenvalues of this tensor are perturbed. We apply this methodology to a convex channel and show that the ensuing eigenvector perturbations are a more accurate measure of uncertainty when compared with a pure eigenvalue perturbation.

1. Introduction

Turbulent flows are present in a wide number of engineering design problems. Due to the disparate character of such flows, predictive methods must be robust, so as to be easily applicable for most of these cases, yet possessing a high degree of accuracy in each. Furthermore, as the processes of analysis and design involve repeated iterations, the predictive method must be computationally economical. Concomitantly, even with the increasing developments in computational hardware and the use of new techniques that enable significant progress on high fidelity simulations of turbulent flows using DNS or LES, Reynolds-average Navier-Stokes (RANS) models are still the main tool employed to solve engineering turbulence problems. The assumptions and simplifications made during the formulation of such RANS closures can limit their ability to account for facets of turbulent physics. This motivates further investigation, as seen in the increase in research activities devoted to error estimation and Uncertainty Quantification (UQ) associated with RANS modeling.

One important tool increasingly in use is the application of data driven techniques for capturing the essential features of the Reynolds stress tensor (RST) computed from a high fidelity source. The works developed by Xiao *et al.* (2016), Wang *et al.* (2016*b*), Ling & Templeton (2015), Ling *et al.* (2016), and Parish & Duraisamy (2016) are examples

† Federal University of Rio de Janeiro, Brazil

of investigations that are applying data driven techniques to infer modeling errors and uncertainties concerning the use of RANS simulations.

Uncertainties in RANS predictions can be classified into aleatoric and epistemic uncertainties. Aleatoric, or statistical, uncertainties are a specific to the system under investigation(e.g., Thompson *et al.* 2016). In contrast, epistemic uncertainty is associated with a lack of adequate representation of the physics of the problem. The origins of this misrepresentation can lie either in lack of knowledge or in the high costs of increasing the fidelity of the physical representation. RANS-based models suffer from an inherent structural inability to replicate fundamental turbulence processes and specific flow phenomena, as they introduce a high degree of epistemic uncertainty into the simulations arising due to the model form.

In this context, a methodology developed by Iaccarino and co-workers (see Emory *et al.* 2013; Gorlé & Iaccarino 2013; Gorlé *et al.* 2014) presented a physics-based, nonparametric approach to estimate the model-form uncertainties. This framework approximates structural variability via sequential perturbations injected into the predicted Reynolds stress eigenvalues, eigenvectors and the turbulent kinetic energy. The eigenvalue perturbation formulation of this approach has been applied to engineering problems with considerable success (Xiao *et al.* 2016; Emory *et al.* 2013).

The starting point for understanding the procedure is to write $\mathbf{R}$ as a function of the turbulent kinetic energy, k; the eigenvalues and eigenvectors of the deviatoric part of the Reynolds Stress tensor, $\mathbf{a}$, is

$$\mathbf{R} = k\left(\frac{1}{3}\mathbf{1} + \mathbf{Q}\boldsymbol{\Lambda}\mathbf{Q}^{\mathbf{T}}\right), \tag{1.1}$$

where $\mathbf{1}$ is the identity tensor, $\mathbf{Q}$ is the orthonormal matrix of the unit eigenvectors of $\mathbf{a}$, and $\boldsymbol{\Lambda}$ is the diagonal matrix of the eigenvalues of $\mathbf{a}$. Then perturbations are introduced in these elements to obtain a final perturbed Reynolds Stress tensor, $\mathbf{R}^*$, of the form

$$\mathbf{R}^* = k^*\left(\frac{1}{3}\mathbf{1} + \mathbf{Q}^*\boldsymbol{\Lambda}^*\mathbf{Q}^{\mathbf{T}*}\right). \tag{1.2}$$

These papers developed a systematic procedure to obtain the perturbed form of the turbulent kinetic energy and the eigenvalues of the normalized Reynolds stress anisotropy tensor, $\mathbf{a}$, defined by

$$\mathbf{a} = \frac{1}{2k}\mathbf{R} - \frac{1}{3}\mathbf{1} = \frac{1}{2k}\mathbf{b}, \tag{1.3}$$

where $\mathbf{b}$ is the deviatoric part of the RST, was developed in these papers. In particular, the eigenvalues of $\mathbf{a}$ are confined to the barycentric map (see Banerjee *et al.* 2007), i.e., the locus of possible values for the eigenvalues of $\mathbf{a}$ within the constraints of realizability (Reynolds Stress is positive definite and the Cauchy-Schwartz inequality is valid). A marker-function based on the angle between the velocity vector and the direction of its variation is used to compute the intensity of the perturbation. The direction of this perturbation inside the barycentric map is an important part of the procedure. In line with the perturbation to the Reynolds stress eignevalues, there have been studies to develop the perturbations to the turbulent kinetic energy (Mishra *et al* 2015, 2016). This is essential to account for the limitations in the modeling of the turbulent transport process in RANS closures.

At a less matured stage is the issue of the perturbation of the eigenvectors of the Reynolds stress anisotropy tensor. Wang *et al.* (2016*a*) first tried to perturb the Reynolds

stress eigenvectors by using Euler angles to fully explore uncertainty space in RANS simulations. Wang *et al.* (2016*b*) then attempted to learn the functional form of discrepancies in Euler angles based on machine learning techniques. Their prediction results showed that the learning performance in eigenvectors is not as satisfactory as that of the eigenvalues, indicating that the Euler angles may not be a suitable way of representing the discrepancy between eigenvector systems.

In the present work, we propose a framework for the eigenvector perturbations. It makes use of the Reynolds stress transport equation to make the eigenvector perturbation consistent with the corresponding eigenvalue perturbations. To this end, the terms that are modeled in the RSTE are estimated from the mean velocity and Reynolds stress tensor fields that are obtained from the RANS model.

2. Methodology

The methodology presented here takes advantage of any usual technique developed to insert an eigenvalue perturbation on the base field of the Reynolds Stress tensor. It consists of a two–stage procedure in which, after the perturbation of the eigenvalues is injected, the corresponding perturbation of the eigenvectors is introduced.

First, we consider the transport equation for the RST

$$\frac{\bar{D}\mathbf{R}}{\bar{D}t} = -\nabla\mathbf{v}\cdot\mathbf{R} - \mathbf{R}\cdot\nabla^T\mathbf{v} + \nu\nabla^2\mathbf{R} + \mathbf{\Gamma}, \tag{2.1}$$

where tensor $\mathbf{\Gamma}$ accounts for the sum of all tensors that need to be modeled, i.e.,

$$\mathbf{\Gamma} = \nabla\cdot\mathfrak{C} + \mathbf{\Pi} - \boldsymbol{\epsilon}, \tag{2.2}$$

where $\mathfrak{C}$ is the triple correlation of the velocity fluctuations, $\mathbf{\Pi}$ is the velocity-pressure-gradient tensor, and $\boldsymbol{\epsilon}$ is the dissipation tensor. To apply the present procedure, we must compute the corresponding evolution for the Reynolds stress anisotropy tensor. After some manipulation, we find that the transport equation for $\mathbf{b}$ is given by

$$\frac{\bar{D}\mathbf{b}}{\bar{D}t} = -\nabla\mathbf{v}\cdot\mathbf{b} - \mathbf{b}\cdot\nabla^T\mathbf{v} + \frac{2}{3}\mathbf{b}:\mathbf{S} + \nu\nabla^2\mathbf{b} + \hat{\mathbf{\Gamma}}, \tag{2.3}$$

where $\hat{\mathbf{\Gamma}} \equiv \mathbf{\Gamma} - \frac{1}{3}\mathrm{tr}\mathbf{\Gamma} + \frac{4}{3}\kappa\mathbf{S}$. Let $\mathbf{b}_a$ and $\mathbf{v}$ be the anisotropy RST and let the velocity fields originate from a RANS model. The procedure can be summarized in the following steps:

(*a*) Use a standard procedure that perturbs the eigenvalues of $\mathbf{a}$ to obtain a distribution of uncertainty on the Reynolds Stress anisotropy tensor, $\Delta\mathbf{b}_{eval}$. Obtain an intermediate RST, $\mathbf{b}_{int} = \mathbf{b}_a + \Delta\mathbf{b}_{eval}$.

(*b*) Compute $\hat{\mathbf{\Gamma}} = \frac{\bar{D}\mathbf{b}_a}{\bar{D}t} + \nabla\mathbf{v}\cdot\mathbf{b}_a + \mathbf{b}_a\cdot\nabla^T\mathbf{v} - \nu\nabla^2\mathbf{b}_a$ from Eq. (2.3) using the modeled Reynolds Stress field.

(*c*) Update mean velocity field by solving the momentum equation for the intermediate RST, $\mathbf{b}_{int}$.

(*d*) Use the RSTE to find a new perturbed RST, $\mathbf{b}_1$.

(*e*) Extract the corresponding eigenvector perturbation, $\Delta\mathbf{b}_{evec}$, with respect to $\mathbf{b}_a$.

(*f*) Find a new RST, $\mathbf{b}^* = \mathbf{b}_a + \Delta\mathbf{b}_{eval} + \Delta\mathbf{b}_{evec}$.

(*g*) Solve momentum equation.

Some variations of the above algorithm can be proposed and will be examined in future works. For instance, one variation is to divide the perturbation $\Delta\mathbf{b}_{eval}$ into smaller steps and keep computing the corresponding eigenvector perturbation during the trajectory. A

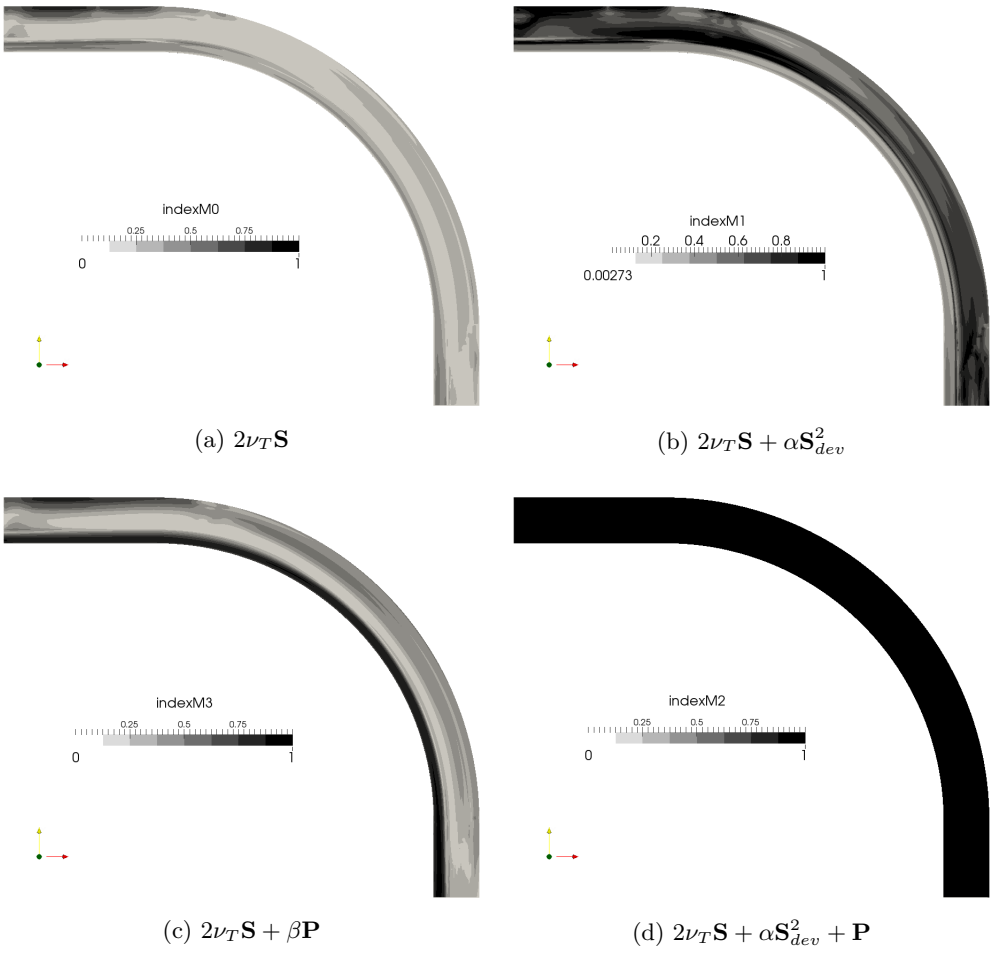

(a) $2\nu_T\mathbf{S}$ (b) $2\nu_T\mathbf{S} + \alpha\mathbf{S}^2_{dev}$

(c) $2\nu_T\mathbf{S} + \beta\mathbf{P}$ (d) $2\nu_T\mathbf{S} + \alpha\mathbf{S}^2_{dev} + \mathbf{P}$

FIGURE 1. Indices of performance associated with the tensor basis considered.

second variation is to feed back the eigenvector perturbation so that one ends on a null additional eigenvalue perturbation.

3. Errors associated with Boussinesq and nonlinear eddy-viscosity models

Our test problem is the convex channel considered by Singh & Duraisamy (2016). They performed LES on this geometry and provided the data corresponding to average quantities with respect to this problem. We have performed a RANS simulation maintaining the main features of the LES carried out by Singh & Duraisamy (2016). As a preliminary result we evaluate how the Boussinesq approximation is able to capture the Reynolds stress tensor that comes from the high fidelity simulations. To this end, we employed the method developed by Thompson *et al.* (2010), i.e., to project the Reynolds stress tensor into the direction of the rate of strain tensor. We have also projected the Reynolds stress tensor into an extended basis of mean kinematic quantities. Thompson (2008) proposed

an index to capture the importance of a tensor (in this case $\mathbf{R_{mod}}$) with respect to a second one (in this case $\mathbf{R_{HF}}$) where the first is an additive part of the second. This scalar index, ϕ, is given by

$$\phi = 1 - \frac{2}{\pi}\cos^{-1}\frac{||\mathbf{R_{mod}}||}{||\mathbf{R_{HF}}||}, \tag{3.1}$$

where $\mathbf{R_{HF}}$ is the RST that comes from a high fidelity simulation, $\mathbf{R_{mod}}$ is the modeled RST, and the symbol $||.||$ represents the norm operator. The construction is such that $\mathbf{R_{HF}} = \mathbf{R_{mod}} + \mathbf{E}$, where $\mathbf{E}$ can be seen as a measure of the error associated with the model.

Figure 1 shows the performance of the Boussinesq hypothesis as well as other nonlinear eddy-viscosity models. These nonlinear eddy-viscosity models are linear combinations of $\mathbf{I}$, $\mathbf{S}$, and $\mathbf{S}^2$, where $\mathbf{S}$ is the rate-of-strain tensor, and the non-persistence-of-straining tensor, $\mathbf{P}$, which represents the local ability of the flow to avoid being persistently stretched (Thompson 2008). From Figure 1(a) we can see that the projection of the RST from the LES data onto the rate-of-strain tensor, the essence of the Boussinesq hypothesis, is low. The performance fields reveal that adding the nonlinear term $\mathbf{S}$ helps the model prediction far from the wall, whereas the inclusion of tensor $\mathbf{P}$ helps to capture the Reynolds stress tensor near the wall. When both tensors are added to the usual Boussinesq linear eddy-viscosity model, a negligible error is found.

4. Eigenvalue perturbations

As shown by Figure 1, the extent of Boussinesq model failure depends upon the local flow physics (see, e.g., Ling & Templeton 2015, for a detailed discussion of localized RANS failure). Ideally, the location, magnitude, and direction of the perturbations should reflect this non-uniform nature of the RANS error. One may employ specialized marker functions based on local flow features to restrict the perturbations to regions where failure of the baseline model can be reasonably expected (Ling & Templeton 2015; Emory *et al.* 2013). However, perturbing the eigenvalues of a Boussinesq model toward a DNS or LES solution can represent a high-dimensional inference problem if the perturbations must be inferred for each spatial point separately. Instead, we use two additional model transport equations for the invariants of the anisotropy tensor, i.e., for the barycentric coefficients C_{1c} and C_{2c}. Note that transport equations for the invariants of $\mathbf{a}$ already exist in the context of return-to-isotropy models (see, e.g., Pope 2000). However, we deal with a baseline eddy-viscosity model that can be erroneous at certain locations but that is able to yield accurate predictions outside these regions. Therefore, the transport equations for C_{1c} and C_{2c} should describe a return-to-eddy-viscosity when the Boussinesq hypothesis is expected to be valid. Our model transport equations are

$$\begin{aligned}
\frac{\mathrm{D}C_{1c}}{\mathrm{D}t} &= a_{1c}\frac{\epsilon}{k}\left(C_{1c}^{(bl)} - C_{1c}\right) + \frac{\partial}{\partial x_i}\left((\nu + \frac{\nu_T}{\sigma_{1c}})\frac{\partial C_{1c}}{\partial x_i}\right) \\
\frac{\mathrm{D}C_{2c}}{\mathrm{D}t} &= a_{2c}\frac{\epsilon}{k}\left(C_{2c}^{(bl)} - C_{2c}\right) + \frac{\partial}{\partial x_i}\left((\nu + \frac{\nu_T}{\sigma_{2c}})\frac{\partial C_{2c}}{\partial x_i}\right).
\end{aligned} \tag{4.1}$$

The $C_{1c}^{(bl)}$, $C_{2c}^{(bl)}$ are the coefficients computed using the eigenvalues of the Boussinesq anisotropy tensor, i.e., from

$$a_{ij}^{(bl)} = -\frac{\nu_T}{k} S_{ij}. \tag{4.2}$$

The model form of Eq. (4.1) is inspired in the lag models of Olsen & Coakley (2001) and Lillard *et al.* (2012), which are extra transport equations for the Reynolds-stress components or the eddy viscosity, to account for non-equilibrium effects. Broadly speaking, equilibrium flows have a timescale much smaller than the mean flow timescale, allowing the turbulence to react quickly to changes in the mean flow. In these type of circumstances, a direct proportionality between the Reynolds stress tensor and the mean strain rate is a reasonable assumption. However, when a flow is not in equilibrium, there is a lag in the response of the turbulence to changes in the mean flow. This lag cannot be accounted for by eddy-viscosity models given that $\overline{u_i' u_j'}$ reacts immediately to changes in S_{ij} and is therefore modeled by Eq. (4.1). If the flow is in equilibrium, Eq. (4.1) will revert to the Boussinesq model.

It was recently argued that the term "equilibrium" is not a well-defined concept and that Boussinesq model failure near a wall is not related to a lag but rather to the deep anisotropy of the turbulence in this region (Spalart 2015). In any case, we view Eq. (4.1) as a means of locally perturbing the Reynolds stress eigenvalues away from the Boussinesq assumption in an intuitive way and potentially toward a more anisotropic state of turbulence. Since we directly model the coefficients of the barycentric map, the effect of the coefficients a_{1c}, a_{2c} on the state of turbulence is easy to understand *a priori.* For instance, if $a_{1c} = 0$, the effectively set $C_{1c} = 0$ and the trajectory in the barycentric map will follow the axi-symmetric contraction border (provided that $a_{2c} > 0$). See Figure 2 for some examples. Note that it is an inequality $a_{1c} \neq a_{2c}$ that drives the trajectory away the most from the Boussinesq assumption. In contrast, for the choice $a_{1c} = a_{2c}$, the trajectory still follows the plane-strain line, as the Boussinesq model does in this case.

One possible use for Eq. (4.1) is to attempt to utilize its predictable behavior simply to bound a DNS/LES or experimental reference using a limited number of simulations. This route is explored in a Bayesian setting. Another option is to find the values for a_{1c} and a_{2c} such that the trajectory in the barycentric map is simply perturbed in the direction of the reference result. Because the LES trajectory will lie left of the plane-strain line, we know beforehand that $a_{1c} > a_{2c}$. Moreover, we can set the boundary conditions of Eq. (4.1) such that near the wall the trajectory will be closer to the LES result. The result is shown in Figure 3. Note that only the direction of the trajectories match. To obtain a better overlap, eigenvector perturbations should be considered as well.

5. Results

To illustrate the importance of the eigenvector perturbations, we performed an *a priori* analysis using RANS and high-fidelity data to evaluate, separately, the impacts of eigenvalue and eigenvector mismatch.

Figure 4 shows the result of this analysis for the convex channel. Firstly, we maintain the eigenvectors obtained from the RANS simulation and matched the eigenvalues provided by the LES data. After that we plug the perturbed RST into the momentum equation to find a new velocity field, $U_{pertEval}$. The difference between the magnitude of this velocity and LES one is shown in figure 4(a). Secondly, we did the opposite pro-

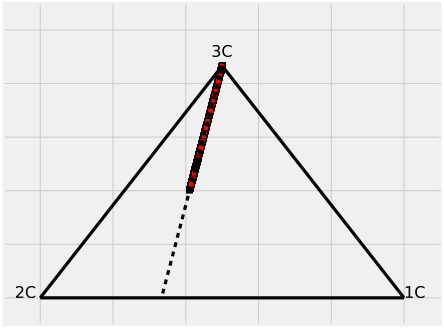

(a) Unperturbed baseline result.

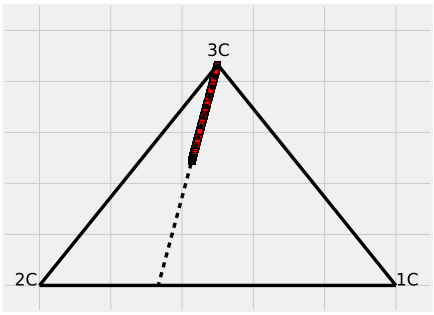

(b) Case 1: $a_{1c} = a_{2c} = 0.35$.

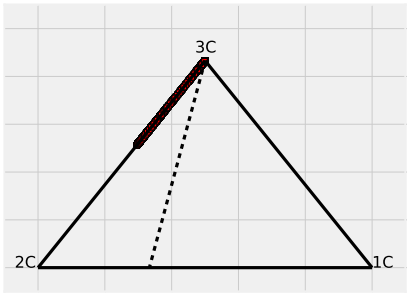

(c) Case 2: $a_{1c} = 0$, $a_{2c} = 0.35$.

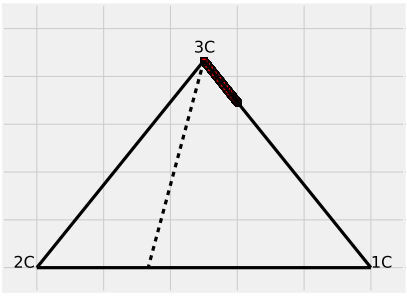

(d) Case 3: $a_{1c} = 0.35$, $a_{2c} = 0$.

FIGURE 2. The trajectories in the barycentric map of the unperturbed model and model (4.1) with three coefficient cases.

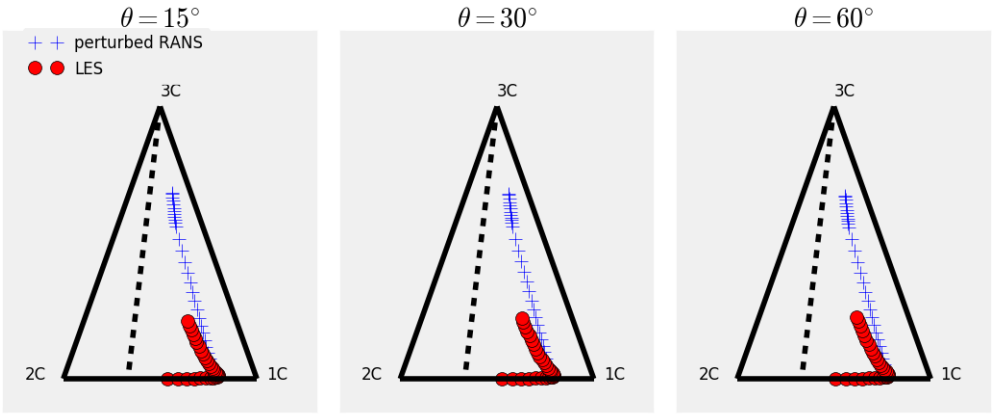

FIGURE 3. Three near-wall trajectories at three angles along the curved section of the channel.

cedure, i.e. we keep the eigenvalues obtained from the RANS simulation and matched the eigenvectors given by the LES results and solved the momentum equation to find a

(a) Eigenvalues perturbation (b) Eigenvector perturbation

FIGURE 4. Magnitude difference between the perturbed RANS velocity and LES velocity.

new velocity field, $U_{pertEvec}$. The discrepancy between the two velocity fields is shown in figure 4(b). This comparison shows how the correct changes in eigenvectors can be more representative of the high fidelity result than the matching of the eigenvalues and serves to motivate the investigation of eigenvector perturbation.

Figure 5, shows the procedure delineated here applied to three different line positions of the domain corresponding to lines at 90^0, 60^0, and 0^0. In each of the figure panels, we see four velocity profiles corresponding to LES (U_{LES}), RANS simulation (U_{RANS}), RANS with perturbed eigenvalues using Eq. (4.1) (U_{val}), and RANS with perturbed eigenvalues and corresponding perturbation of eigenvectors (U_{tot}). Notably, the RANS simulation does give a result similar to the one provided by the LES. The results obtained from the procedure for the eigenvalue perturbation have shown quite different behavior from the others. The additional eigenvector perturbation that was proposed in the present work brought the velocity profile back to the tendency exhibited by LES and RANS results. These are preliminary results that need further investigation. Given that the RANS velocity profile is not so discrepant from the LES profile, the uncertainties concerning the application of the RANS model in this case are low. In this sense, the eigenvalue perturbation approach used here overestimates the predicted uncertainty with respect to the RANS model. However, the additional corresponding eigenvector perturbation induces a return to the previous levels of uncertainties whose magnitudes can be grasped by the difference between RANS and LES results.

6. Conclusions

We have employed the Reynolds stress transport equations in order to constrain the eigenvector perturbations associated with the Reynolds stress anisotropy tensor in the context of Uncertainty Quantification of RANS modeling. We have employed the procedure to the convex channel considered by Singh & Duraisamy (2016) to test the concept. To this end, we ran a RANS simulation on the same geometry and conditions and used the eigenvalue perturbation technique. Because the present methodology is in a very early stage of development, conclusions are preliminary. We have found that the eigenvalue perturbation alone can lead to an overestimation of the uncertainty with respect

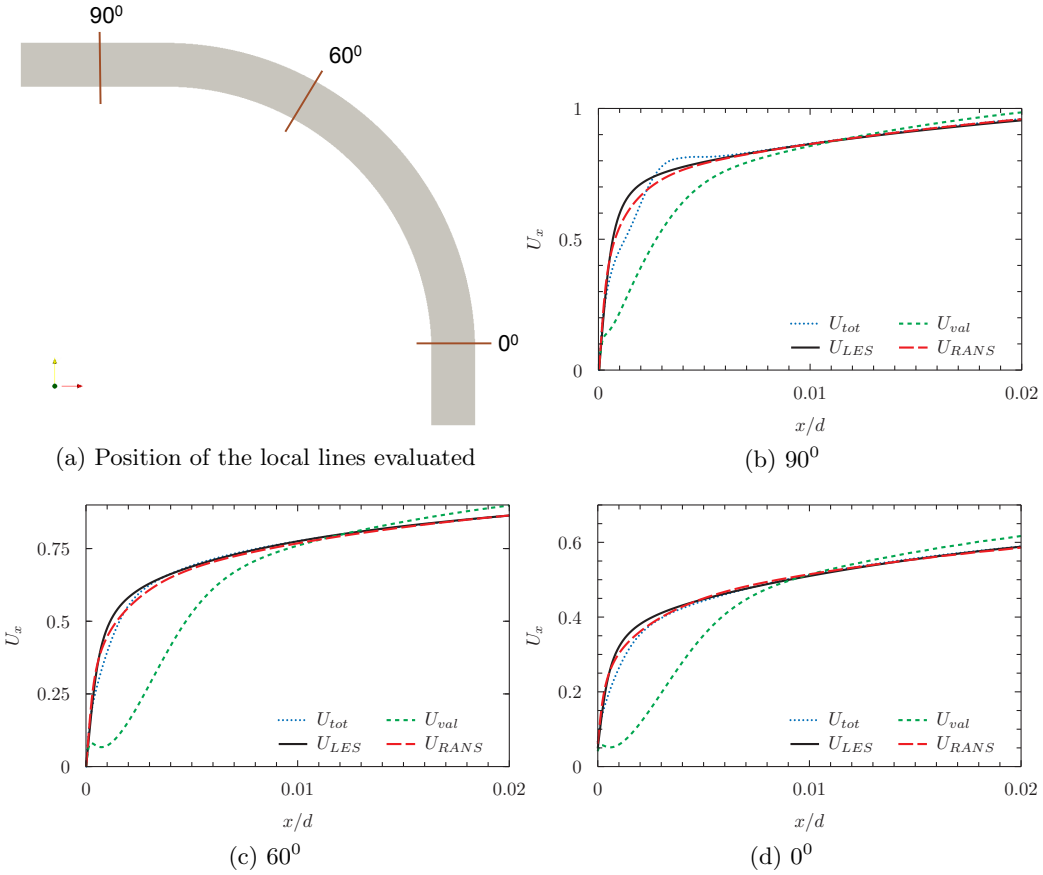

(a) Position of the local lines evaluated (b) 90^0

(c) 60^0 (d) 0^0

FIGURE 5. Velocity profiles corresponding to four cases: LES, RANS, RANS with perturbed eigenvalues (U_{val}), RANS with perturbed eigenvalues and eigenvectors (U_{tot})

to the RANS modeling and that the inclusion of the eigenvector perturbation can induce a more consistence measure of uncertainty, taking the difference between the LES and RANS results as an estimation of the uncertainty.

Acknowledgments

We acknowledge Heng Xiao, Jin-Long Wu, and Jiang-Xu Wang for valuable discussions on the subject during the CTR summer program. We also thank Anand Singh and Karthik Duraisamy for providing the data for the convex channel, and the Center for Turbulence Research for the financial support during this investigation.

REFERENCES

BANERJEE, S., KRAHL, R., DURST, F. & ZENGER, C. 2007 Presentation of anisotropy properties of turbulence, invariants versus eigenvalue approaches. *J. Turbul.* **8**, 1–27.

EMORY, M., LARRSON, J. & IACCARINO, G. 2013 Modeling of structural uncertainties in Reynolds-Averaged Navier-Stokes closures. *Phys. Fluids* **25**, 110822.

GORLÉ, C. & IACCARINO, G. 2013 A framework for epistemic uncertainty quantification

of turbulent scalar flux models for Reynolds-Averaged Navier-Stokes simulations. *Phys. Fluids* **25**, 055105.

Gorlé, C., Larrson, J., Emory, M. & Iaccarino, G. 2014 The deviation from parallel shear flow as an indicator of linear eddy-viscosity model inaccuracy. *Phys. Fluids* **26**, 051702.

Lillard, R., Oliver, A., Olsen, M., Blaisdell, G. & Lyrintzis, A. 2012 The lagRST model: a turbulence model for non-equilibrium flows. *AIAA Paper* 2012-444.

Ling, J., Jones, R. & Templeton, J. 2016 Machine learning strategies for systems with invariance properties. *J. Comput. Phys.* **318**, 22–35.

Ling, J. & Templeton, J. 2015 Evaluation of machine learning algorithms for prediction of regions of high Reynolds averaged Navier Stokes uncertainty. *Phys. Fluids* **27**, 085103.

Olsen, M. & Coakley, T. 2001 The lag model, a turbulence model for non equilibrium flows. In *AIAA Computational Fluid Dynamics Conference, 15 th, Anaheim, CA*.

Parish, E. & Duraisamy, K. 2016 A paradigm for data-driven predictive modeling using field inversion and machine learning. *J. Comput. Phys.* **305**, 758–774.

Pope, S. B. 2000 *Turbulent Flows*. Cambridge University Press.

Singh, A. P. & Duraisamy, K. 2016 Using field inversion to quantify functional errors in turbulence closures. *Phys. Fluids* **28**, 045110.

Mishra, A.A., Iaccarino, G. & Duraisamy, K. Epistemic uncertainty in statistical Markovian turbulence models. *Annual Research Briefs*, Center for Turbulence Research, Stanford University, pp. 183–195.

Mishra, A.A., Iaccarino, G. & Duraisamy, K. Sensitivity of flow evolution on turbulence structure. Phys. Rev. Fluids **1**, 052402.

Spalart, P. 2015 Philosophies and fallacies in turbulence modeling. *Prog. Aero. Sci.* **74**, 1–15.

Thompson, R. L. 2008 Some perspectives on the dynamic history of a material element. *Int. J. Eng. Sci.* **46**, 524–549.

Thompson, R. L., Mompean, G. & Thais, L. 2010 A methodology to quantify the non-linearity of the Reynolds stress tensor. *J. Turbul.* **11**, 1–27.

Thompson, R. L., Sampaio, L. E. B., de Bragança Alves, F. A. V., Thais, L. & Mompean, G. 2016 A methodology to evaluate statistical errors in DNS data of plane channel flows. *Comput. & Fluids* **130**, 1–7.

Wang, J.-X., Sun, R. & Xiao, H. 2016*a* Quantification of uncertainties in turbulence modeling: A comparison of physics-based and random matrix theoretic approaches. *Int. J. Heat and Fluid Flow*.

Wang, J.-X., Wu, J. & Xiao, H. 2016*b* Using data to improve Reynolds stresses in RANS simulations: A physics-informed machine learning approach. Submitted. Available at https://128.84.21.199/abs/1606.07987.

Xiao, H., Wu, J.-L., Wang, J.-X., Sun, R. & Roy, C. J. 2016 Quantifying and reducing model-form uncertainties in Reynolds-Averaged Navier-Stokes simulations: An open-box, physics-based, Bayesian approach. *J. Comput. Phys.* **324**, 115–136.